Spontaneous fracture at expanding phase transformation.

Spontant brott vid expanderande fasomvandling, SMD 2013. Orationem Meam.

Ståhle, P.

SMD 2013

Spontant brott vid expanderande fasomvandling

P. Ståhle
Lunds tekniska högskola, Lund, Sverige

N. Lalanne-Aulet
Institut Francais de Mecanique Avancee, Clermont-Ferrand, France

R. N. Singh and S. Benerjee
BARC, Atomic Research Centre, Mumbai, India

Zr-H solid solution and hydride

Hydrogen occupies tetrahedral sites in Zr-H solid solution

α-lattice distorts to match the γ and δ structures

Interstitial ordering results in periodic occupation of tetrahedral sites

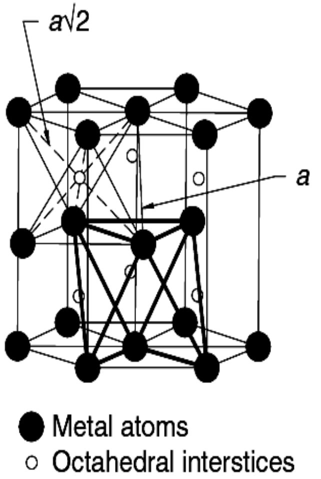

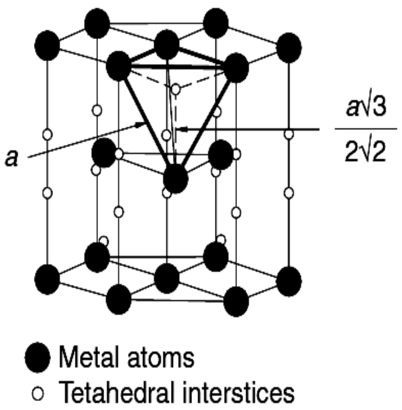

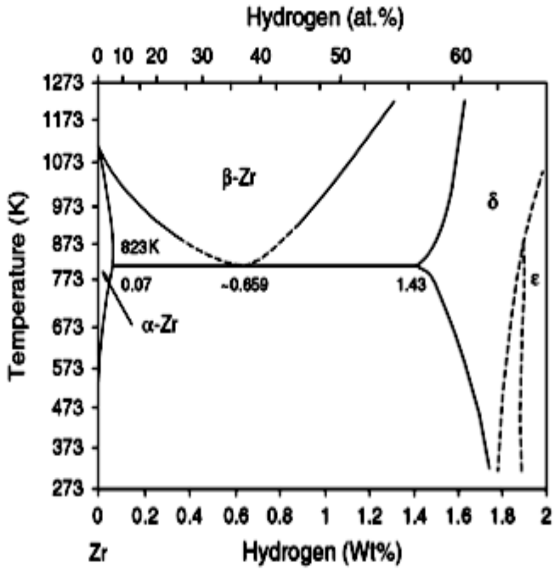

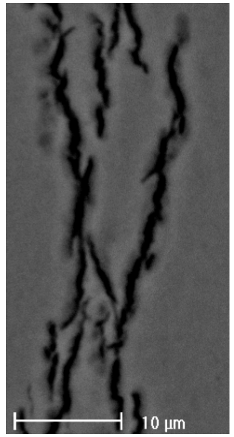

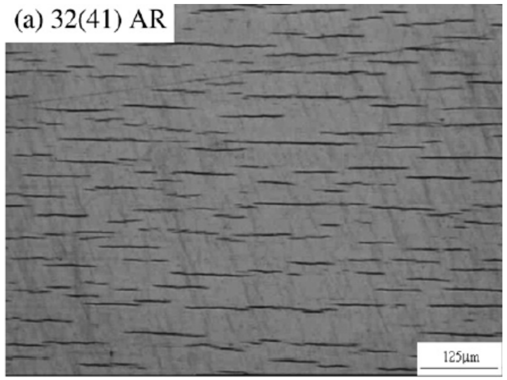

Zr exhibits two allotropic modification: low T hcp (α) and high T bcc (β) phases

Two stable hydrides (δ and ε) and one metastable (γ) hydride forms in this system

Under optical microscope the traces of hydrides appears as dark lines

At higher magnification the hydride plates reveal several smaller entities

Hydride plate comprises of platelets stacked side by side

Each platelet comprises of sub-platelets stacked end to end

Multi-scale Structural Mechanics

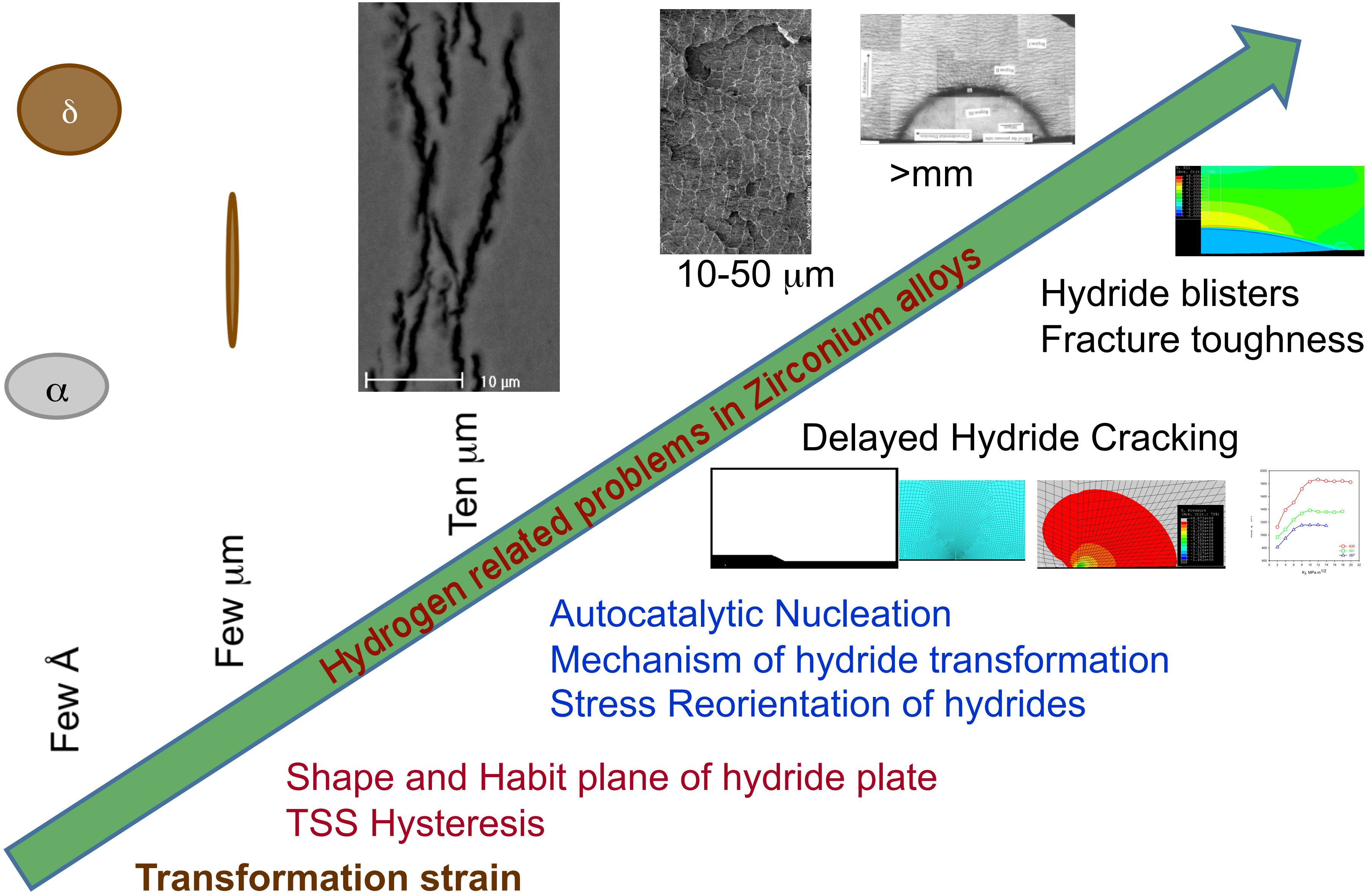

Experimental setup

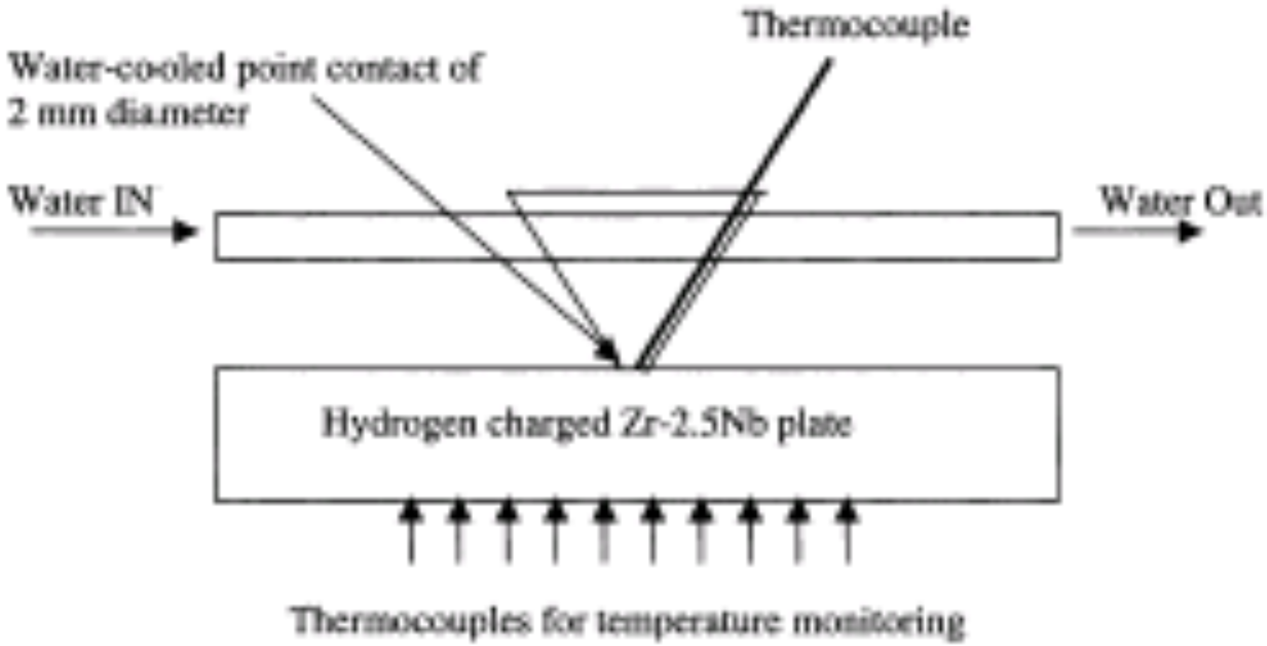

Top view of
hydride blister

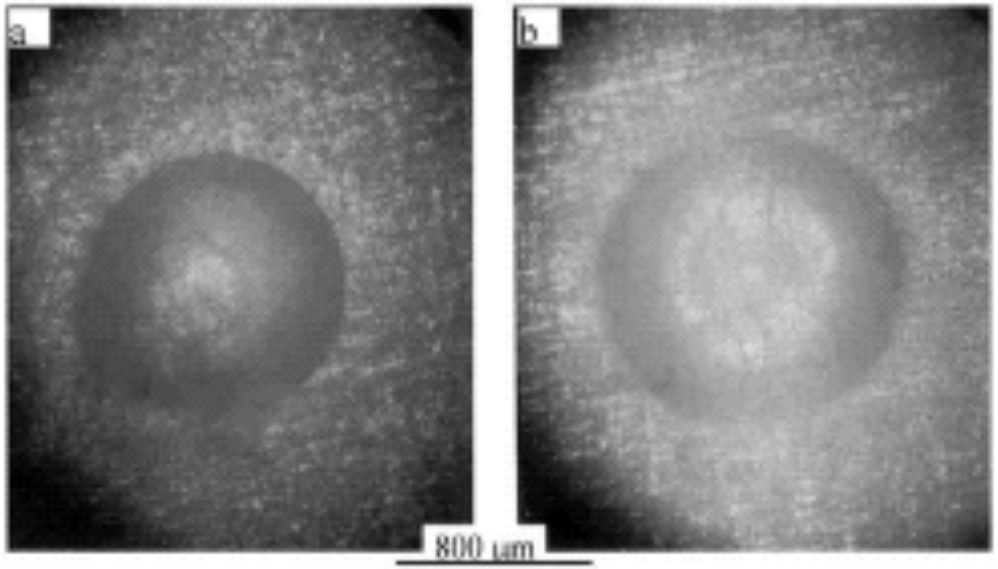

Top view of a hydride blister grown in Zr–2.5wt%Nb pressure tube alloy (Singh *et al*., 2001)

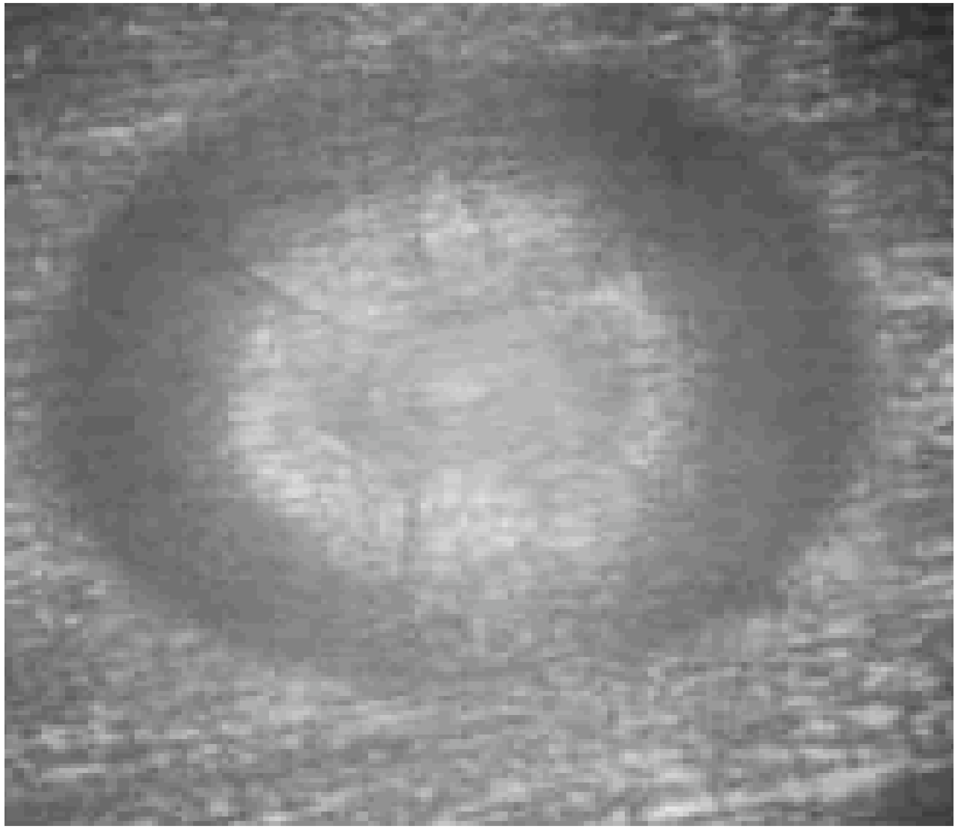

Examination of a section of blister (grown in Laboratory)

Figure : Optical micrograph of hydride blister section, grown in Zr-2.5wt.% Nb pressure tube material. Three regions - Region I - matrix & circumferential hydrides, region II - matrix containing both radial and circumferential hydrides and region III - mainly of δ-hydride.

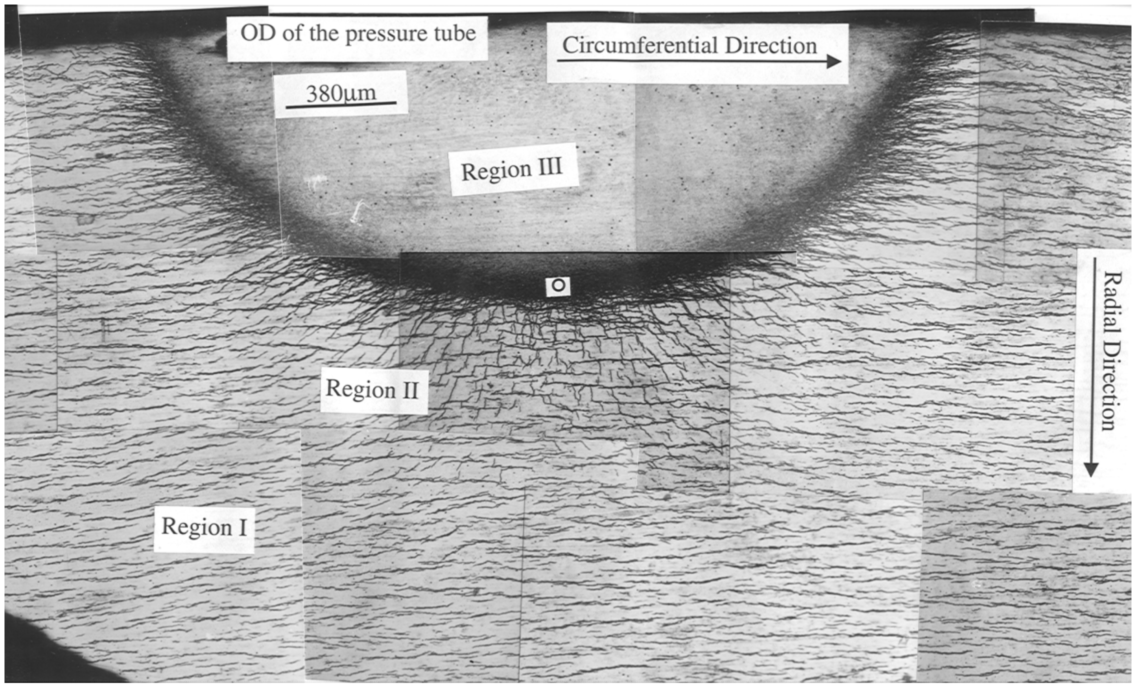

Expanding elastic-plastic inclusion (Hill, 1950)

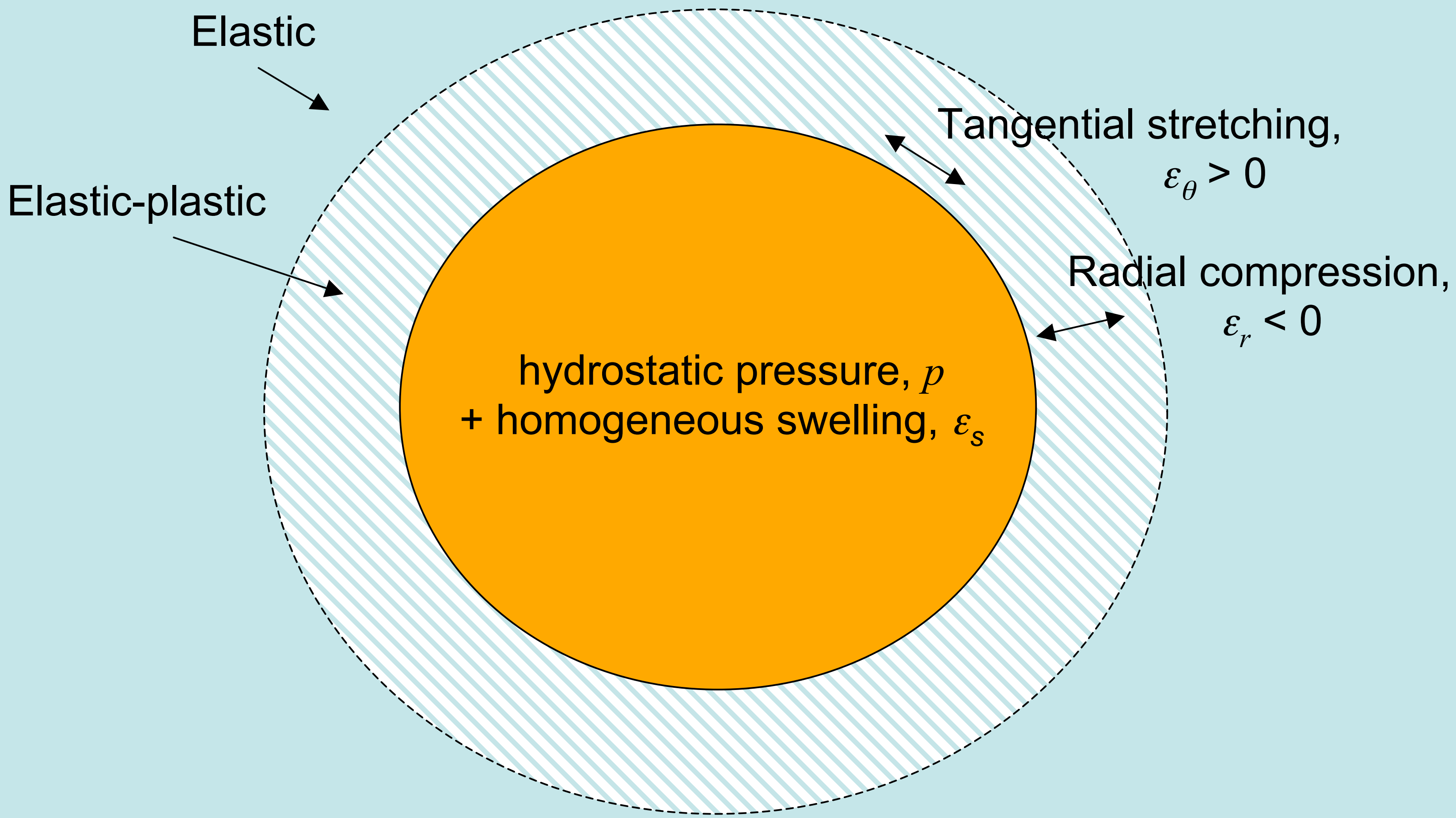

Thin layer increasing inclusion volume (and mass)

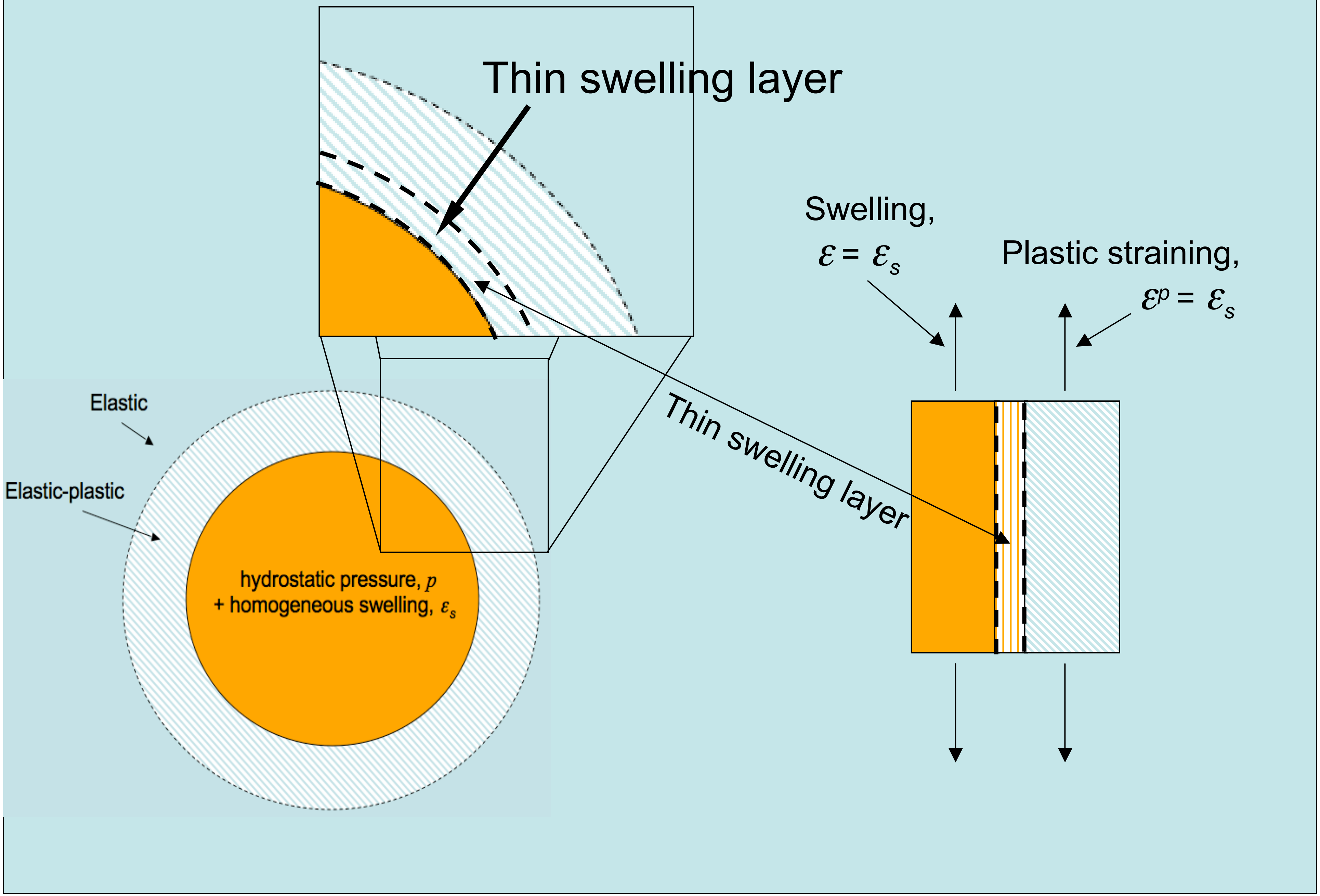

Blister formation - Stress field computation – Multi step

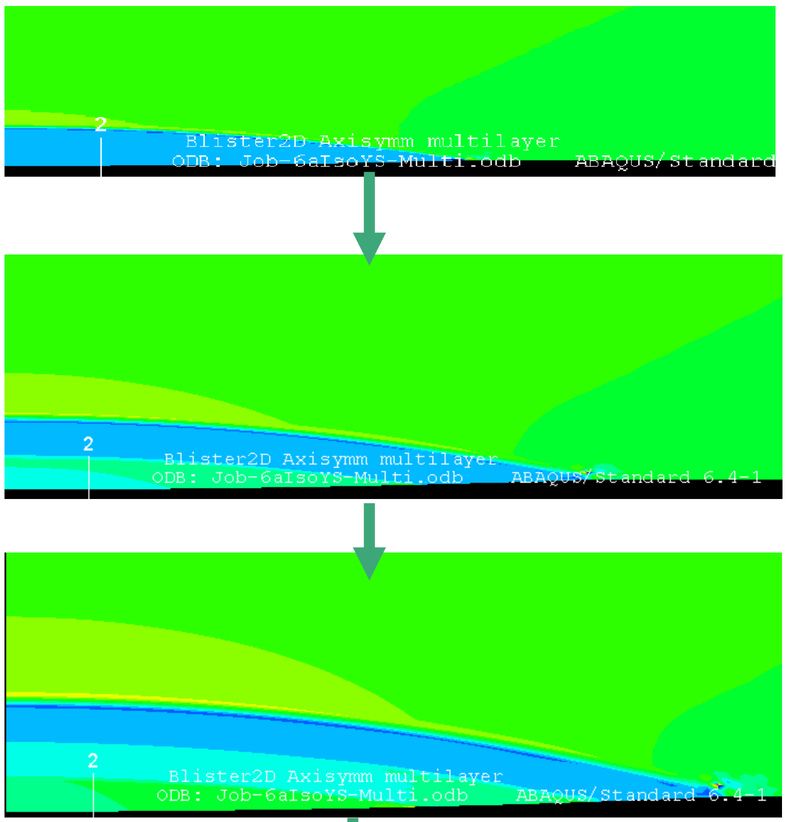

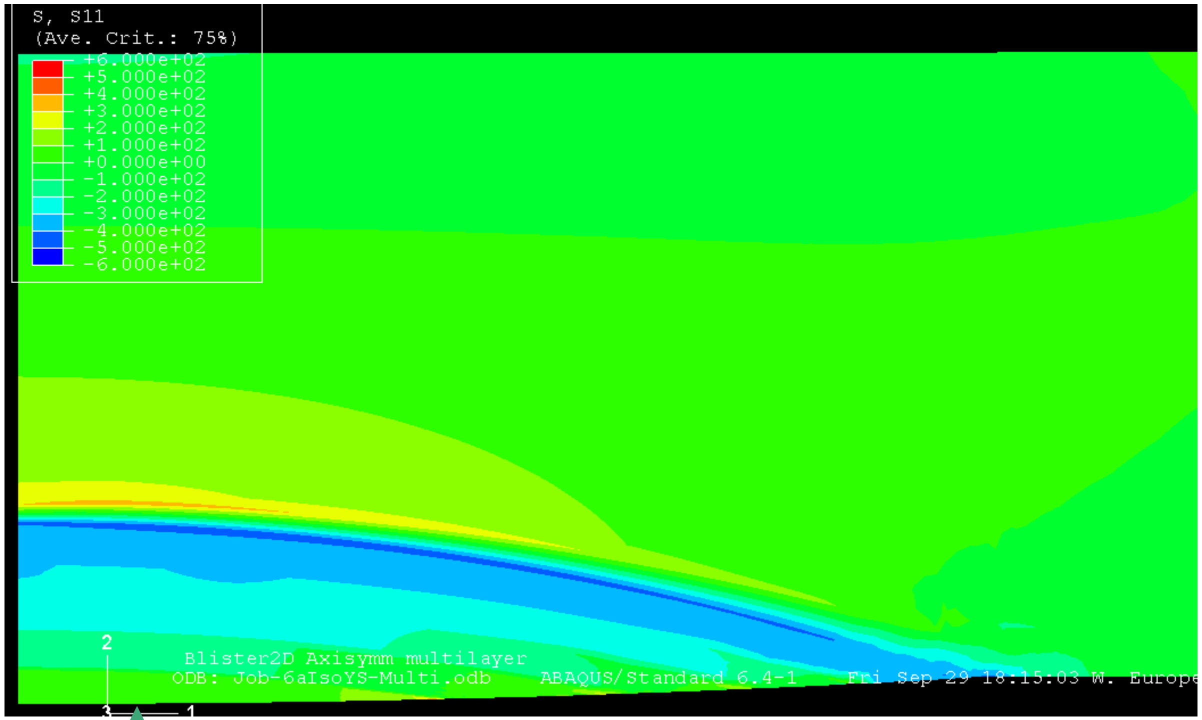

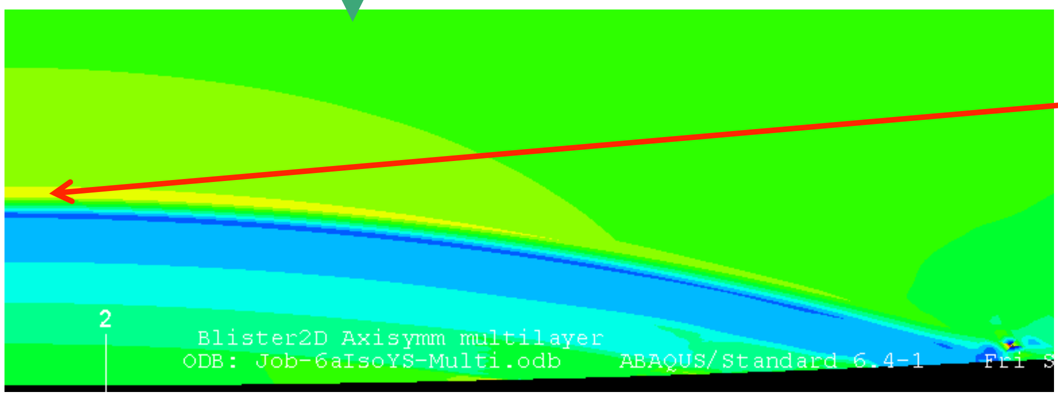

Multi-step transformation in 5 steps
Expansion achieved by raising temperature
Max tensile stress near the deepest point

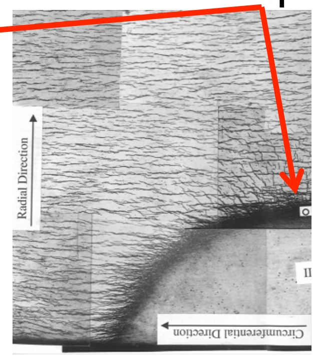

Essential result of FEM and present solution

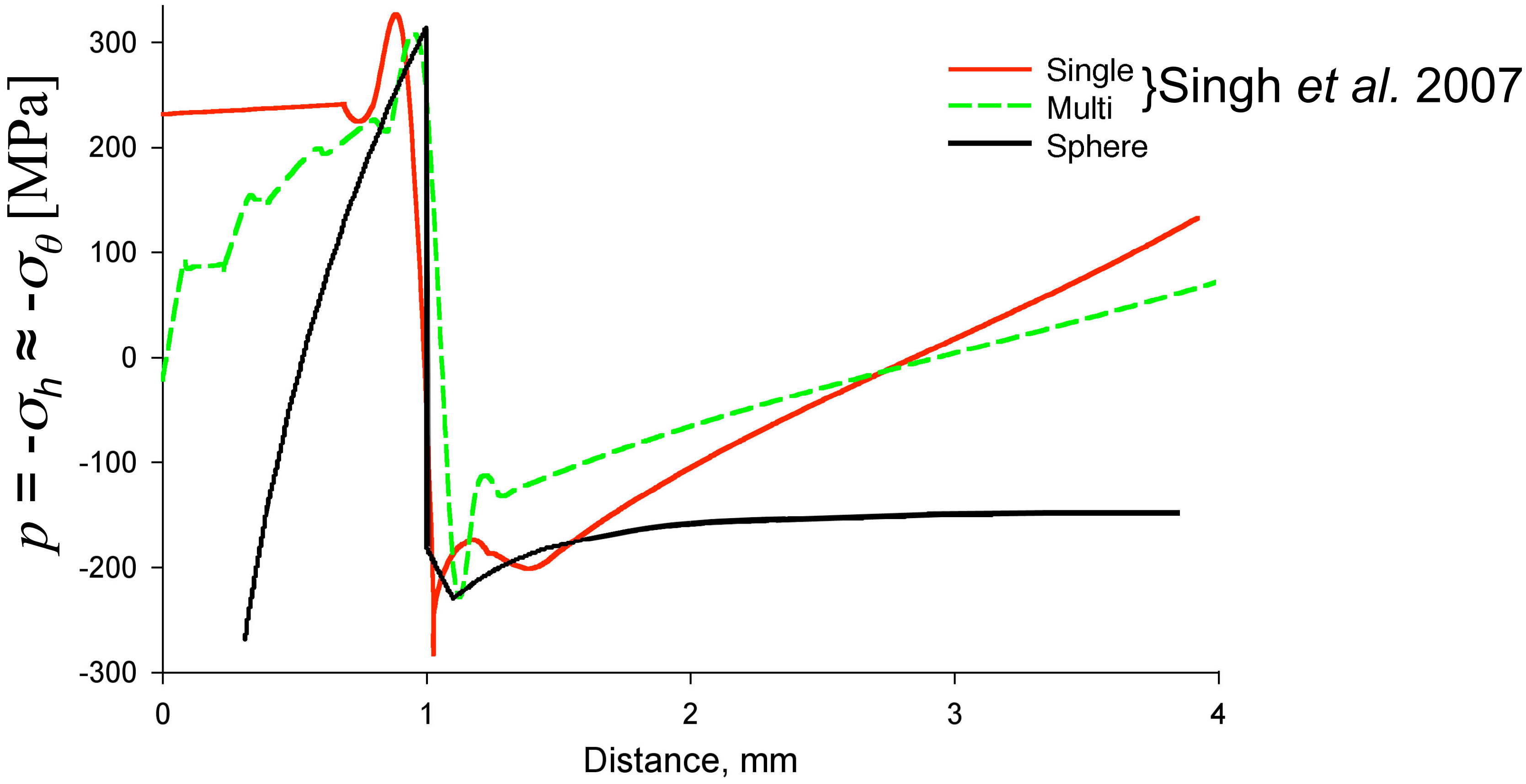

Strains

$$\epsilon_r = \frac{\partial u_r}{\partial r}, \quad \epsilon_\theta = \frac{1}{r}\frac{\partial u_\theta}{\partial \theta} + \frac{u_r}{r},$$
$$\epsilon_{r\theta} = \frac{\partial u_\theta}{\partial r} - \frac{u_\theta}{r} + \frac{1}{r}\frac{\partial u_r}{\partial \theta}.$$

Equilibrium

$$\frac{\partial \sigma_r}{\partial r} + \frac{1}{r}\frac{\partial \sigma_{r\theta}}{\partial \theta} + \frac{1}{r}(2\sigma_r - \sigma_\theta - \sigma_\psi + \sigma_{r\theta}\cot\theta) = 0.$$

$$\frac{\partial \sigma_{r\theta}}{\partial r} + \frac{1}{r}\frac{\partial \sigma_\theta}{\partial \theta} + \frac{1}{r}[(\sigma - \sigma_\psi)\cot\theta + 3\sigma_{r\theta}] = 0.$$

Decomposed strains

$$\epsilon_r = \epsilon_r^e + \epsilon_r^p + \epsilon^s,$$
$$\epsilon_\theta = \epsilon_\theta^e + \epsilon_\theta^p + \epsilon^s,$$
$$\epsilon_\psi = \epsilon_\psi^e + \epsilon_\psi^p + \epsilon^s \text{ and } \epsilon = \epsilon_{r\theta}^e + \epsilon_{r\theta}^p$$

Plast. strain prop. to deviatoric stress

$$\frac{\epsilon_r^p}{\sigma_r - \sigma_h} = \frac{\epsilon_\theta^p}{\sigma_\theta - \sigma_h} = \frac{\epsilon_\psi^p}{\sigma_\psi - \sigma_h} = \frac{\epsilon_{r\theta}^p}{\sigma_{r\theta}},$$

DE:
$$\frac{d^2u_r}{dr^2} + 2\frac{du_r}{r\,dr} - 2\frac{u_r}{r^2} - \frac{1-2\nu}{1-\nu}\left(\frac{d\epsilon^p}{dr} + 3\frac{\epsilon^p}{r}\right) = 0$$

Displacements:
$$u_r = \epsilon_s r - \frac{2(1-2\nu)}{3}\left(1 + 3\ln\frac{r_p r}{R^2}\right)\frac{\sigma_o r}{E} \quad \text{in } r \leq \text{R}.$$

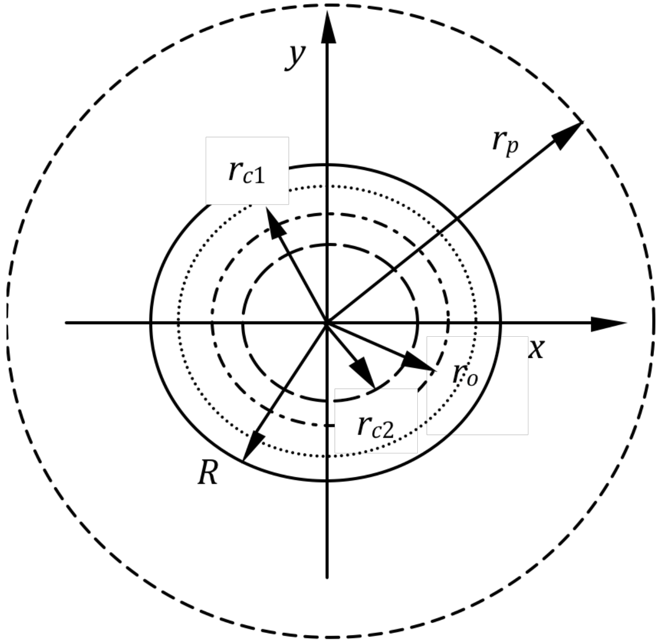

Fig. 2 Different characteristic regions of the solution. In $r > r_p$ the material is elastic; in $r \leq r_p$ the material is plastic; in $r_{c1} < r < R$ no tensile stress; in $r_o < r < r_{c1}$ tensile radial stress; in $r_{c2} < r < r_o$ tensile radial stress and hydrostatic stress; in $r < r_{c2}$ all stresses are tensile.

$$r < r_{c1} = \frac{R^2}{r_p e^{1/3}}, \quad r < r_o = \frac{R^2}{r_p e^{2/3}} \quad \text{and} \quad r < r_{c2} = \frac{R^2}{r_p e^{5/6}}$$

Essential result of FEM and present solution

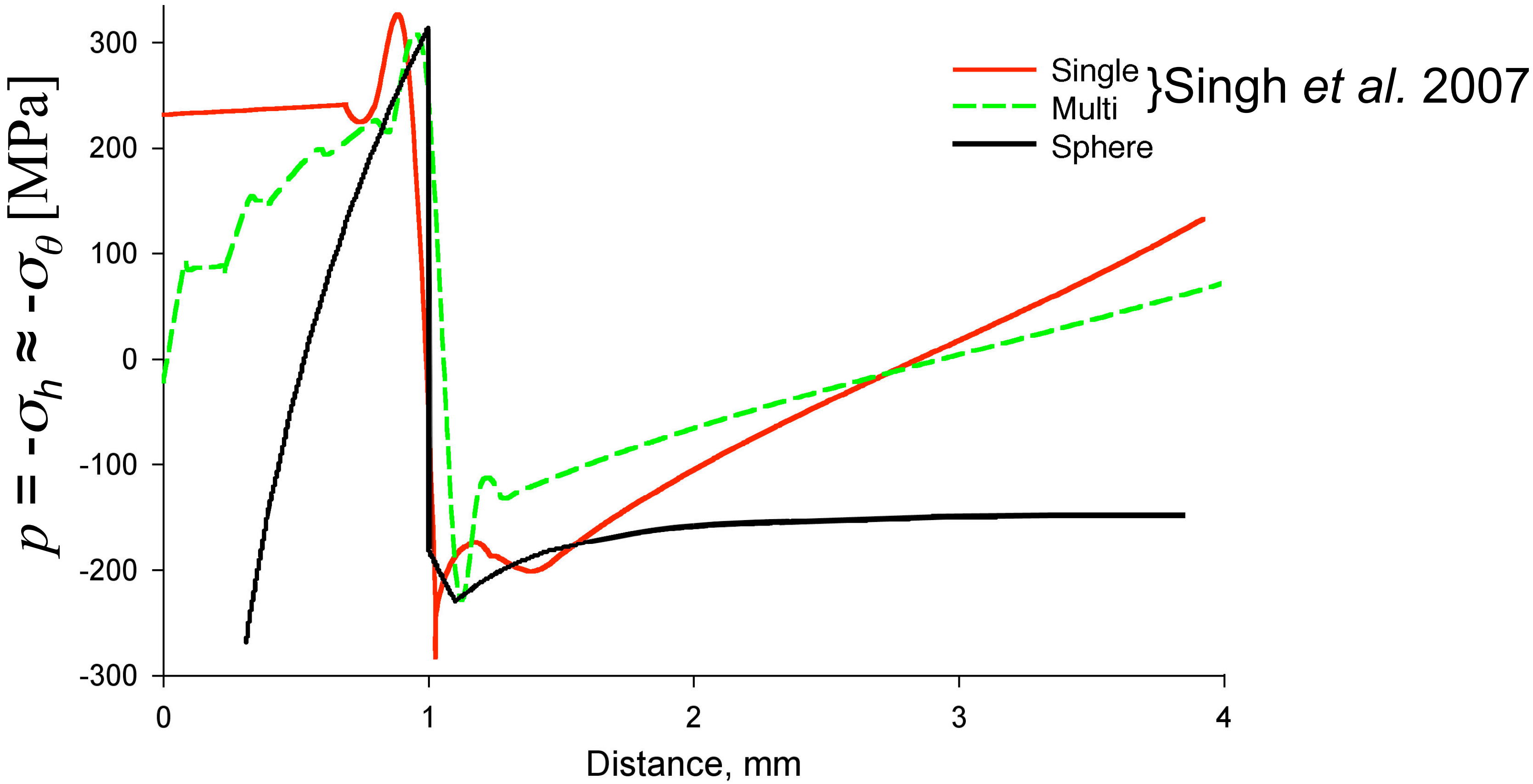

Radial pressure, $-\sigma_r/k$, versus vs. distance r/R

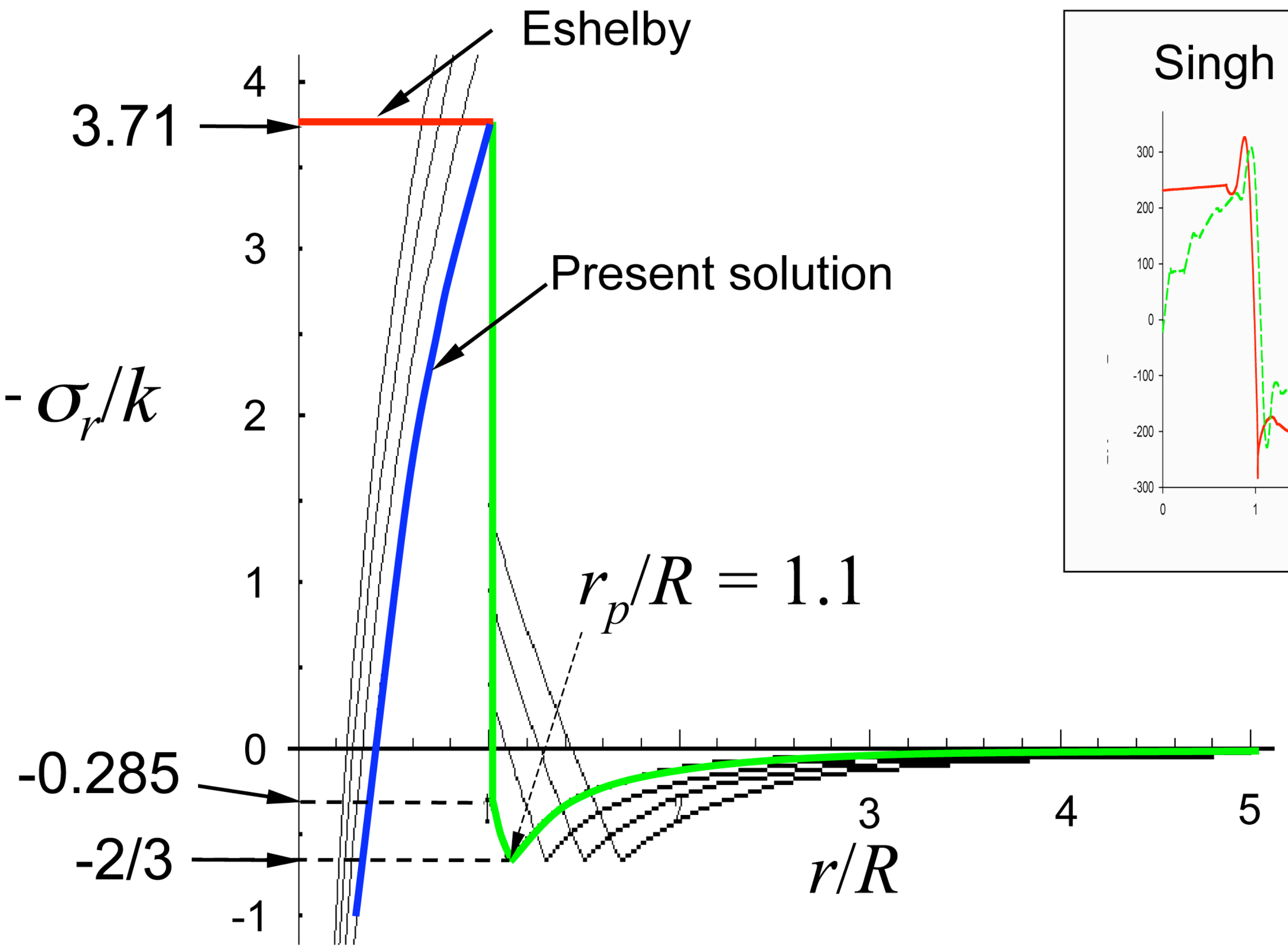

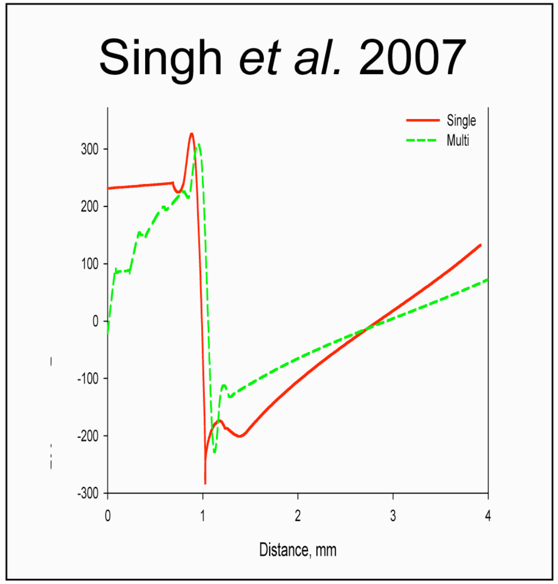

Hoop Stress

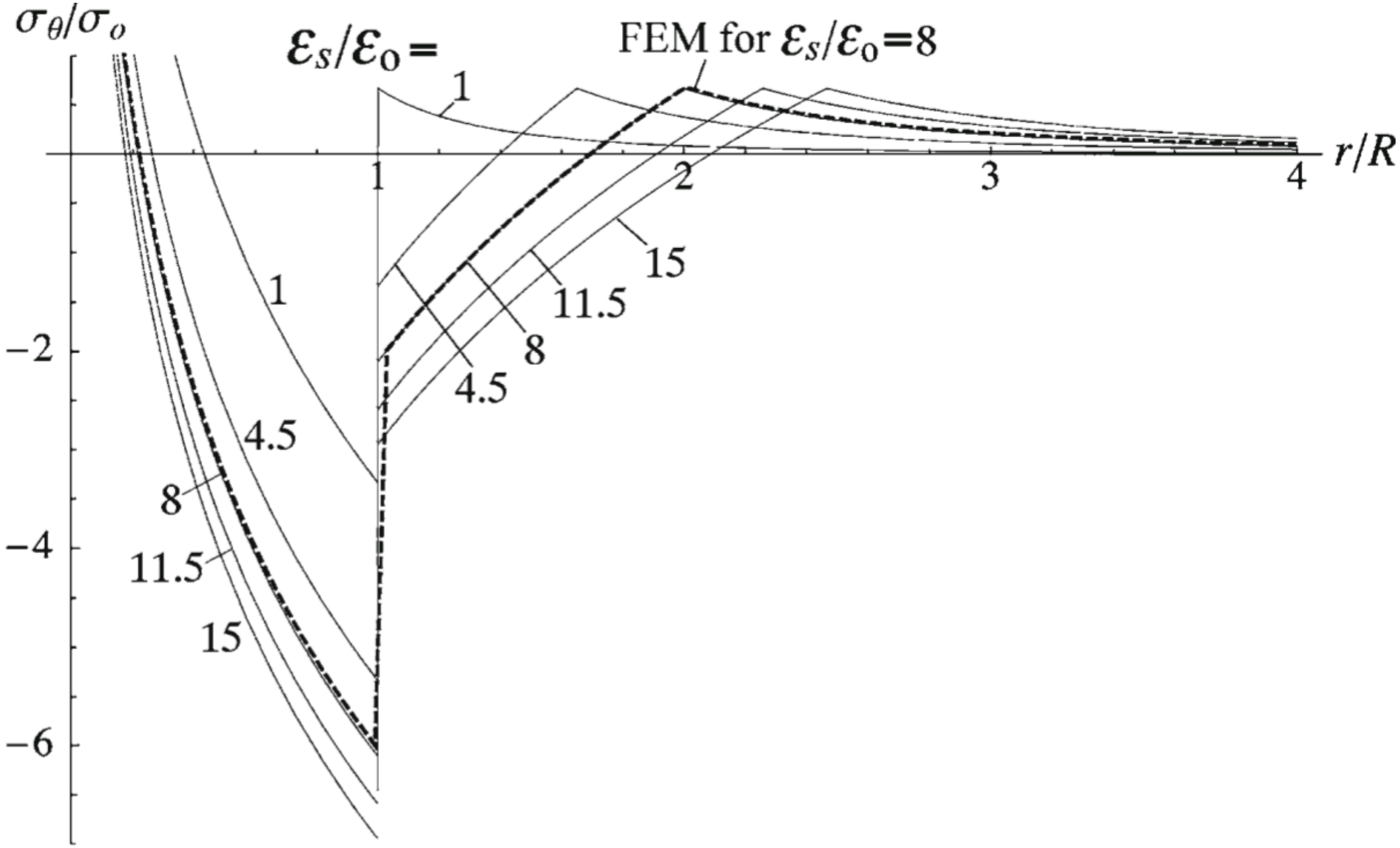

σ_θ/σ_o
$\varepsilon_s/\varepsilon_0 =$
FEM for $\varepsilon_s/\varepsilon_0$=8
1
1
4.5
8
11.5
15
4.5
8
11.5
15
−2
−4
−6
1
2
3
4
r/R

Radial Displacement

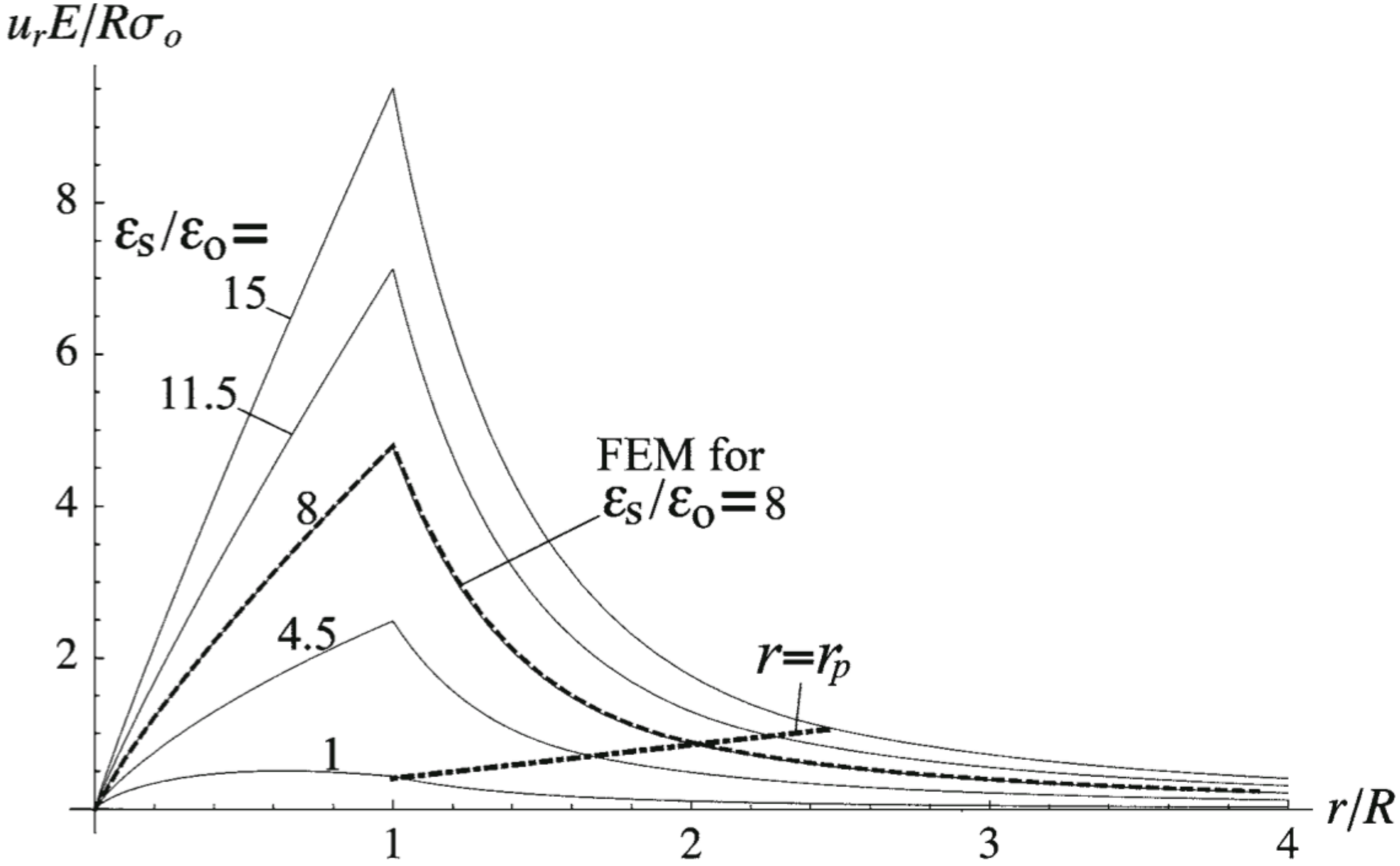

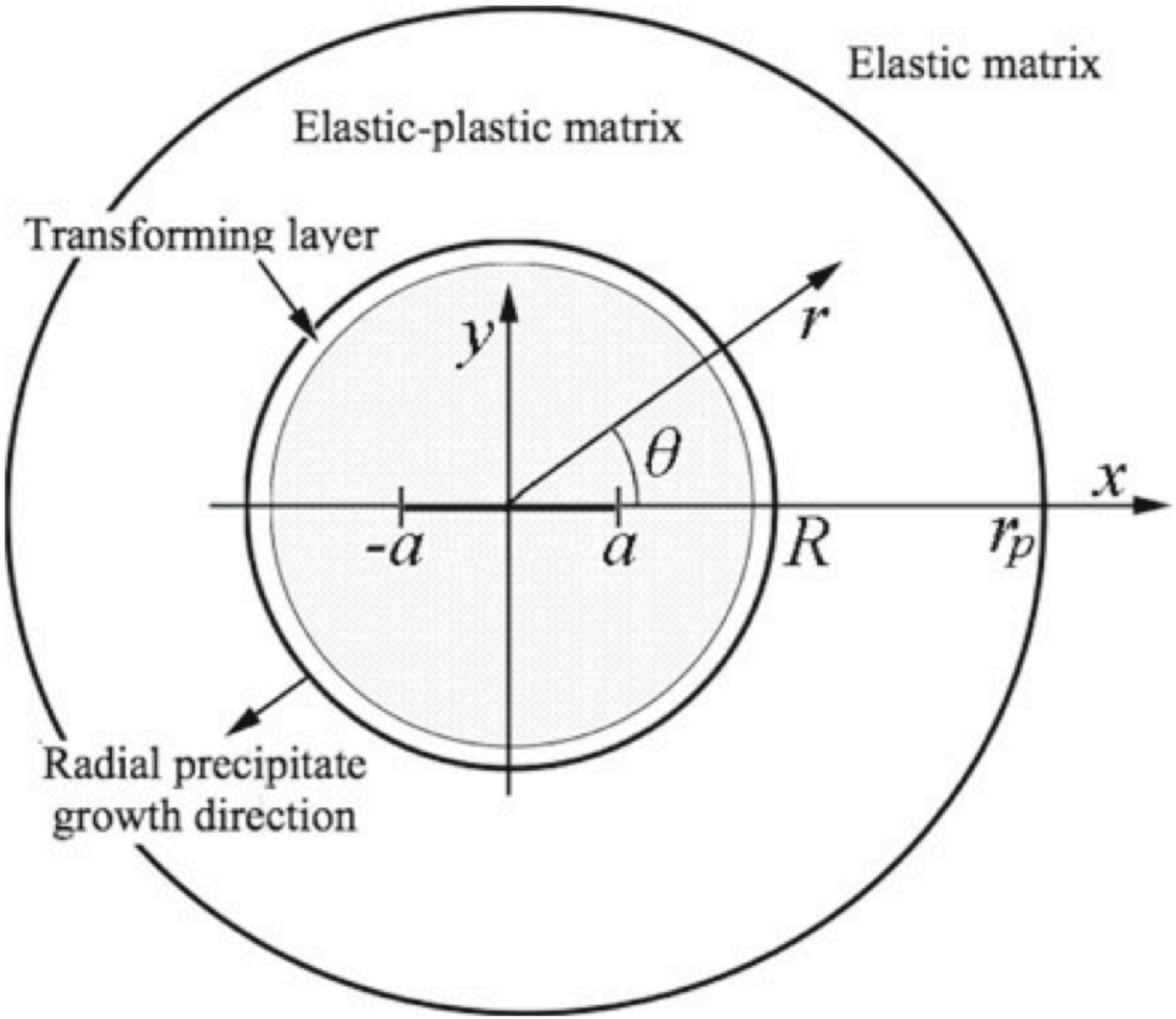
Elastic matrix
Elastic-plastic matrix
Transforming layer
y
r
θ
x
-a
a
R
r_p
Radial precipitate
growth direction

Hoop Stress

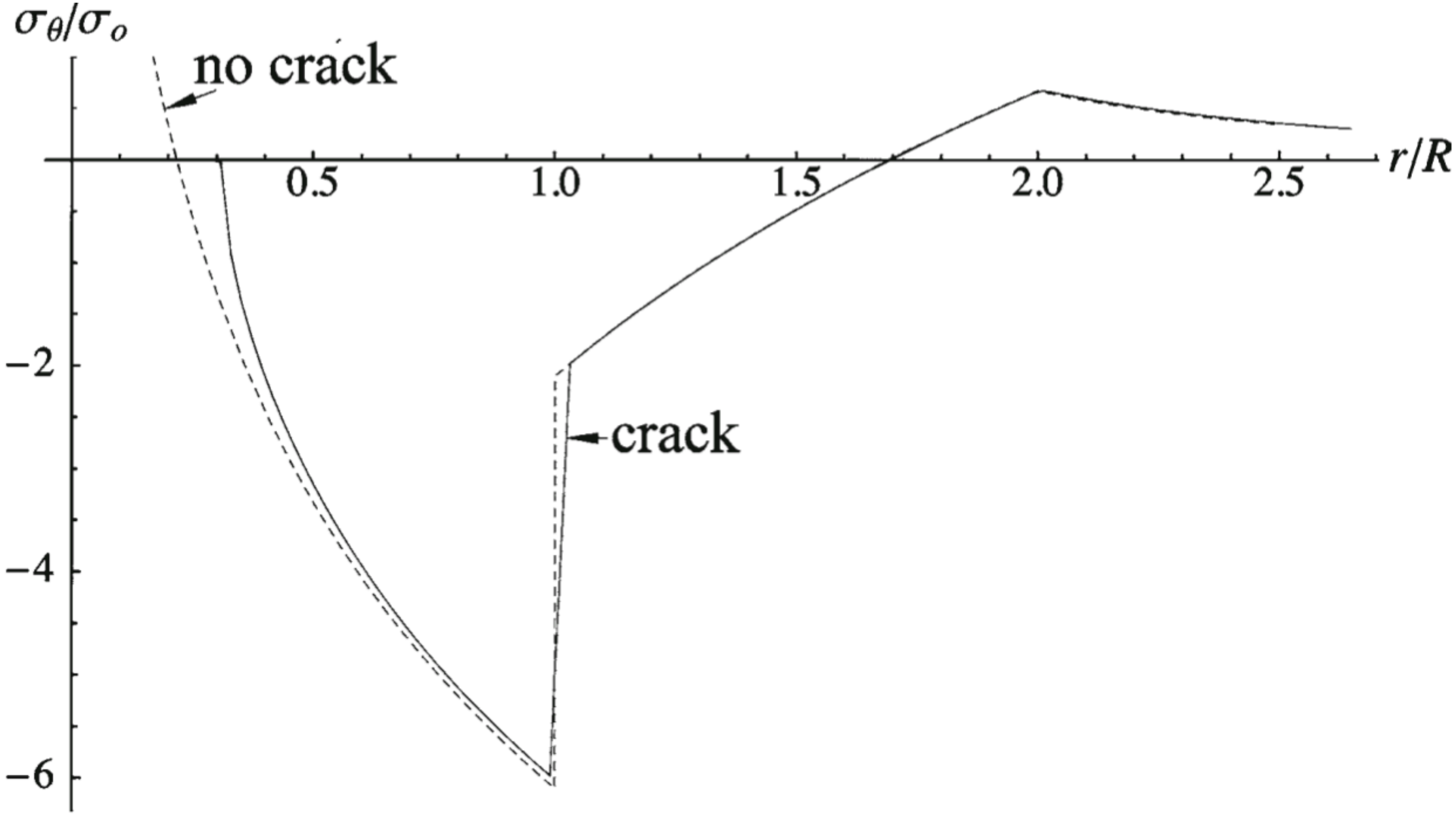

Crack Surface Displacement

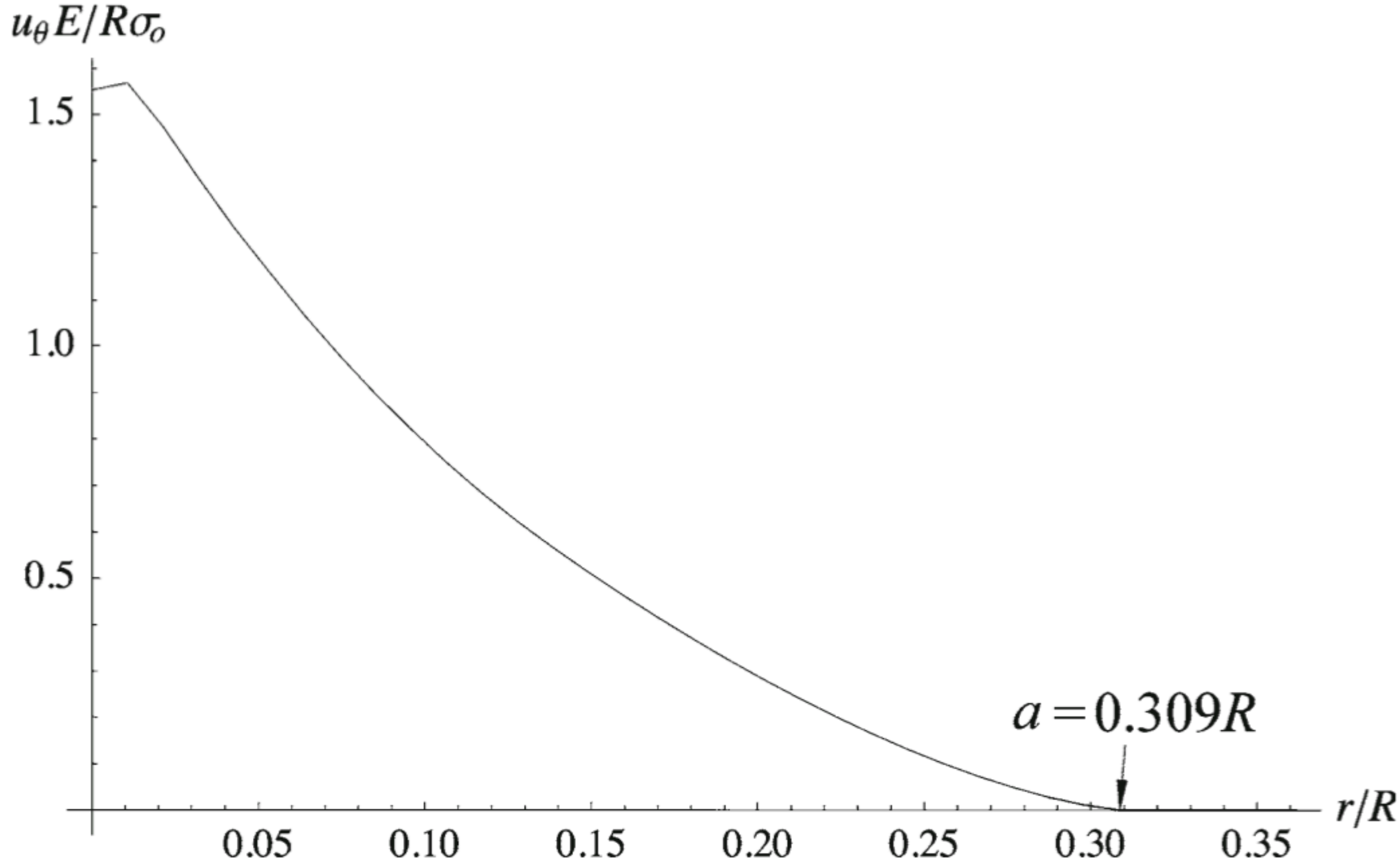

Crack Length vs. Inclusion Radii

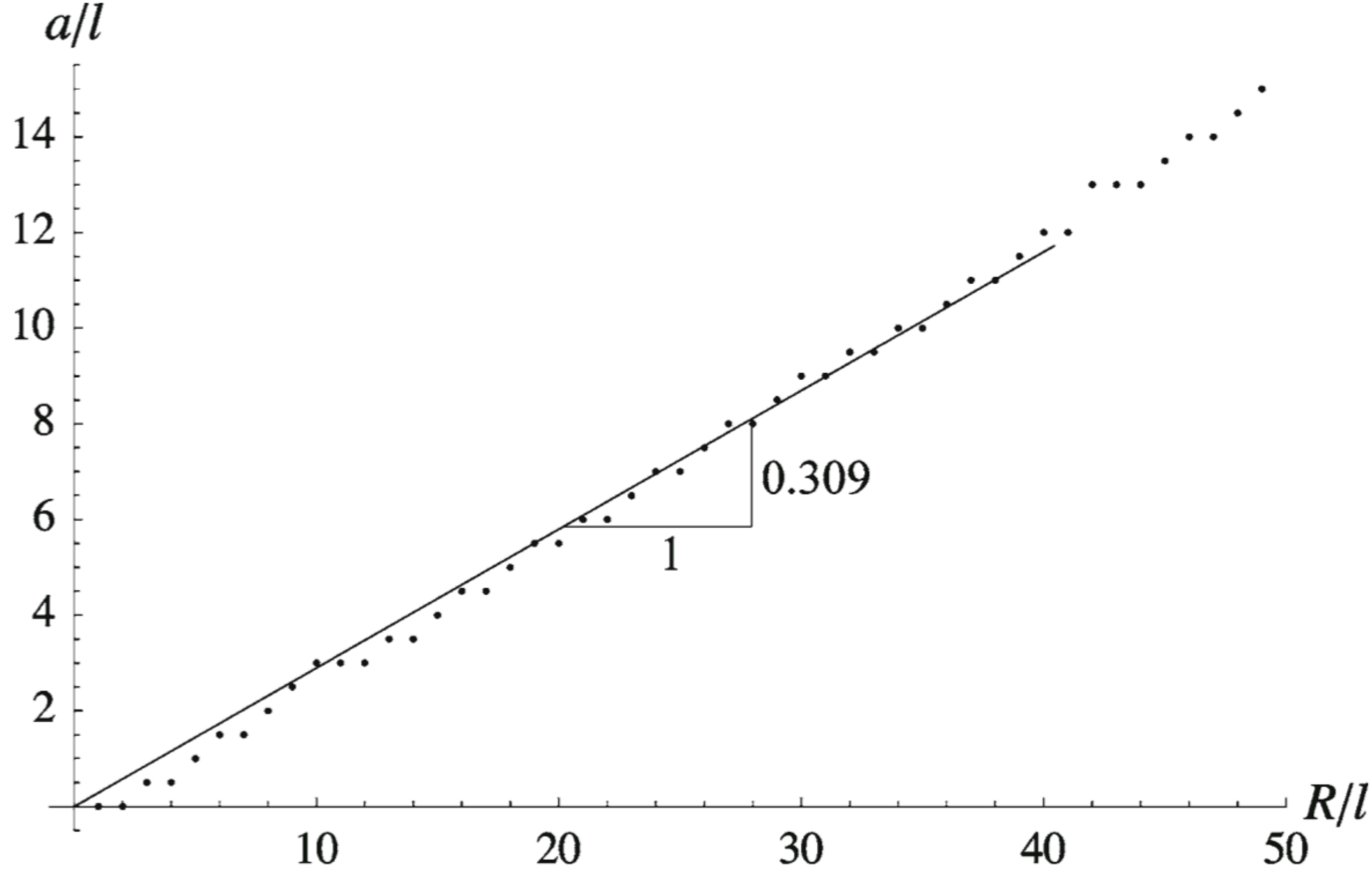

v Mises Stress, Incremental Growth
Expanding Cylinder ahead of a Crack

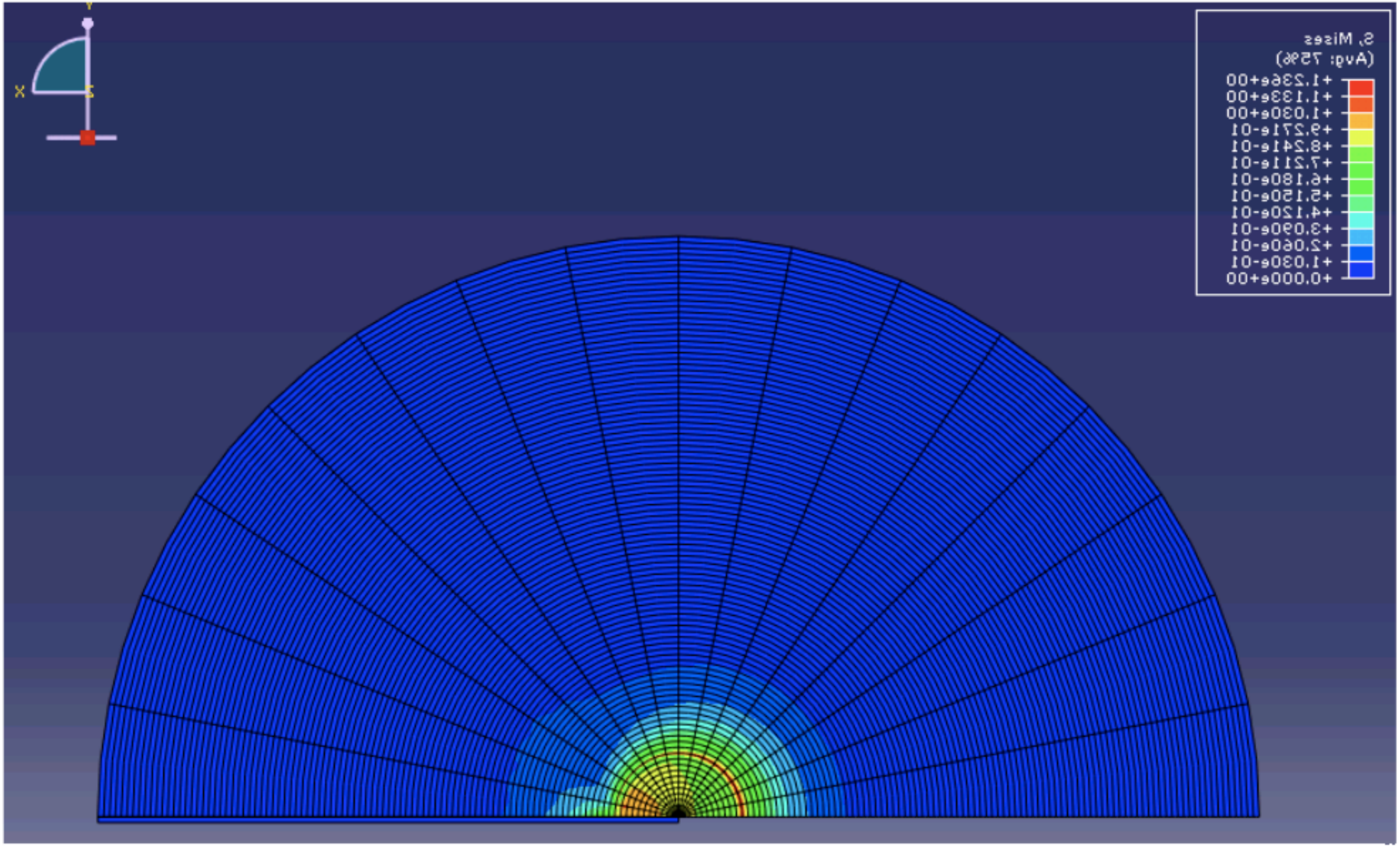

Deformation, Simultaneous Growth
Expanding Cylinder ahead of a Crack

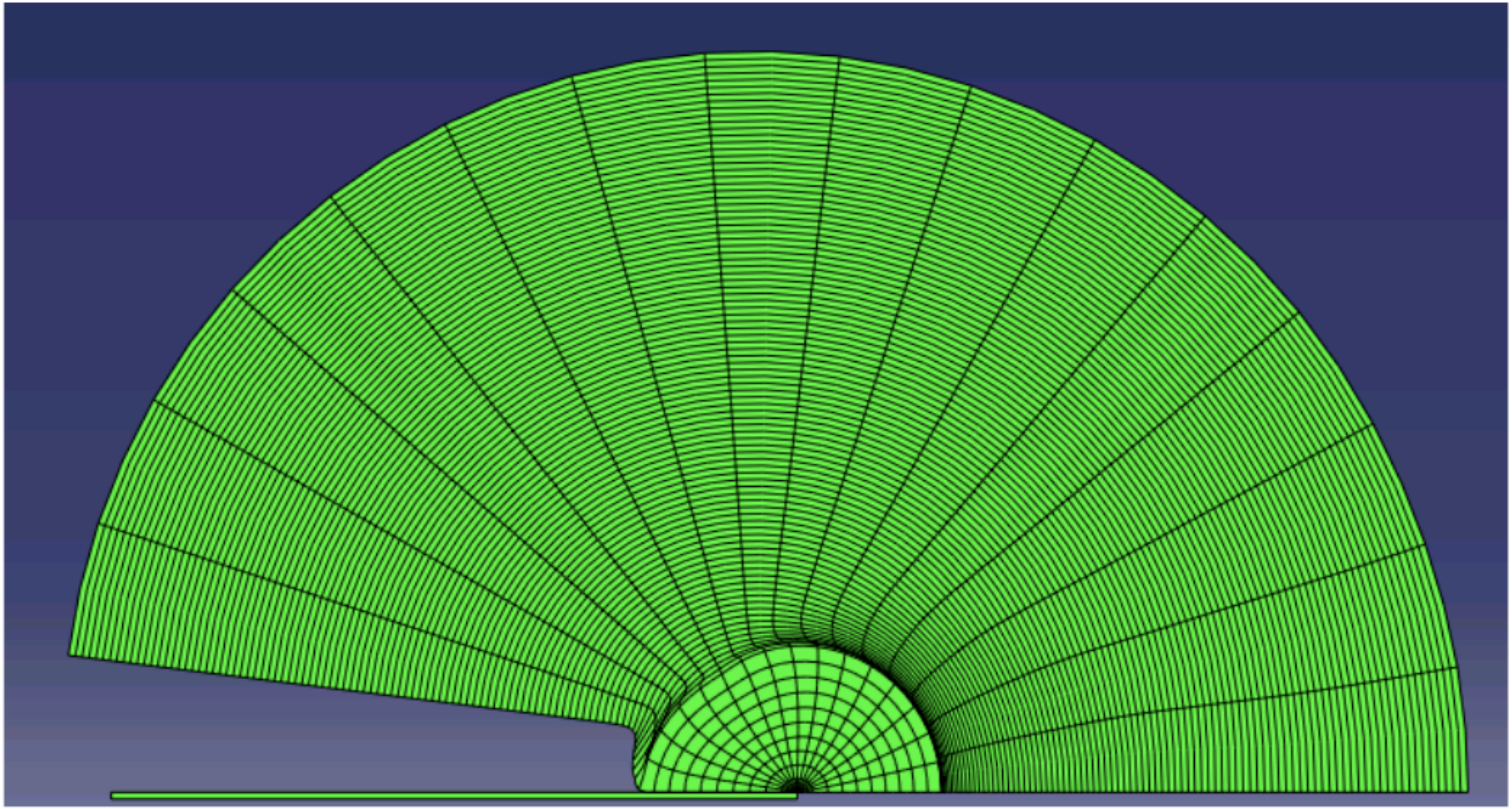

Deformation, Incremental Growth

Expanding Cylinder ahead of a Crack

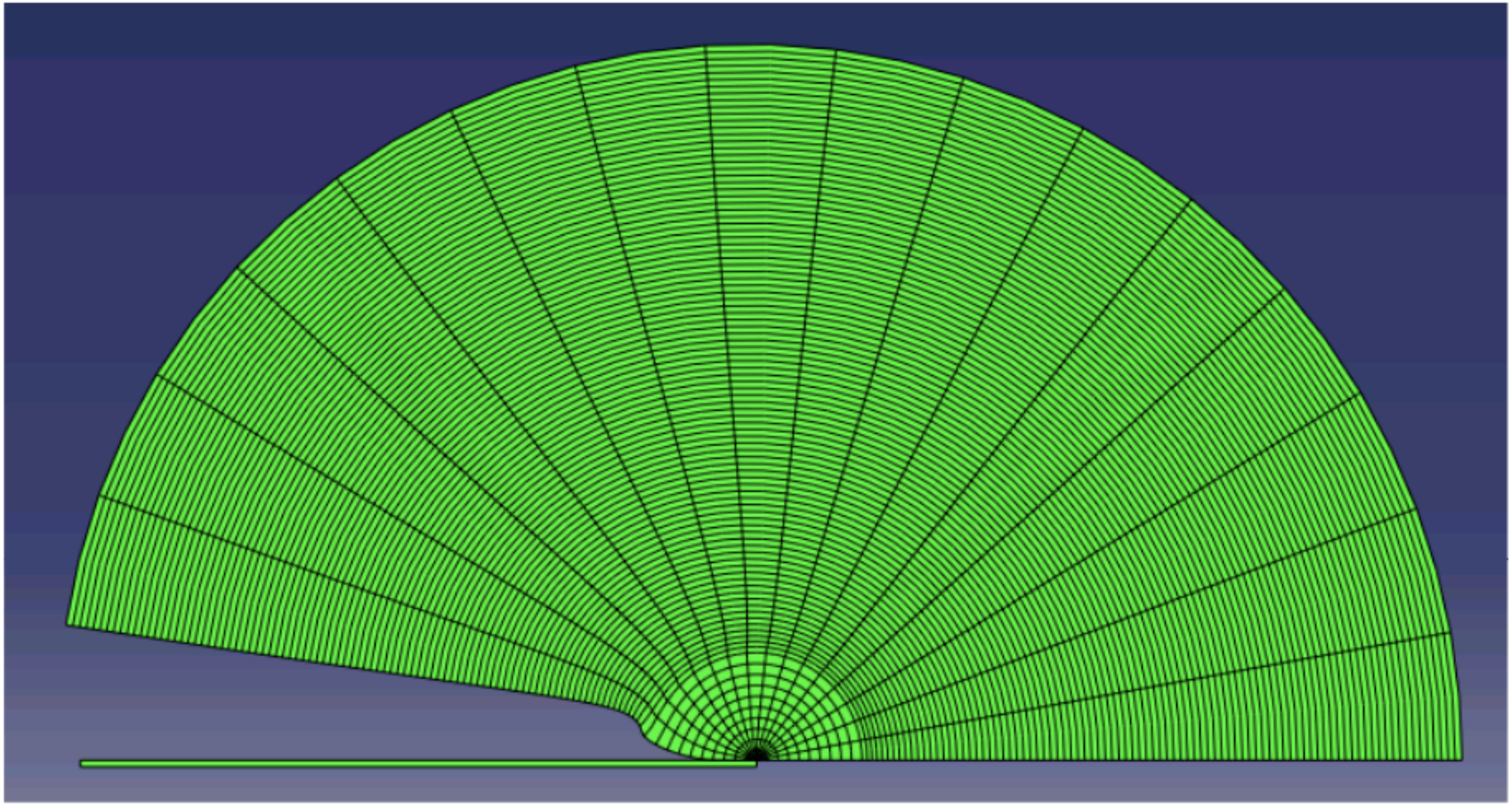

v Mises Stress, Simultaneous Growth
Expanding Cylinder ahead of a Crack

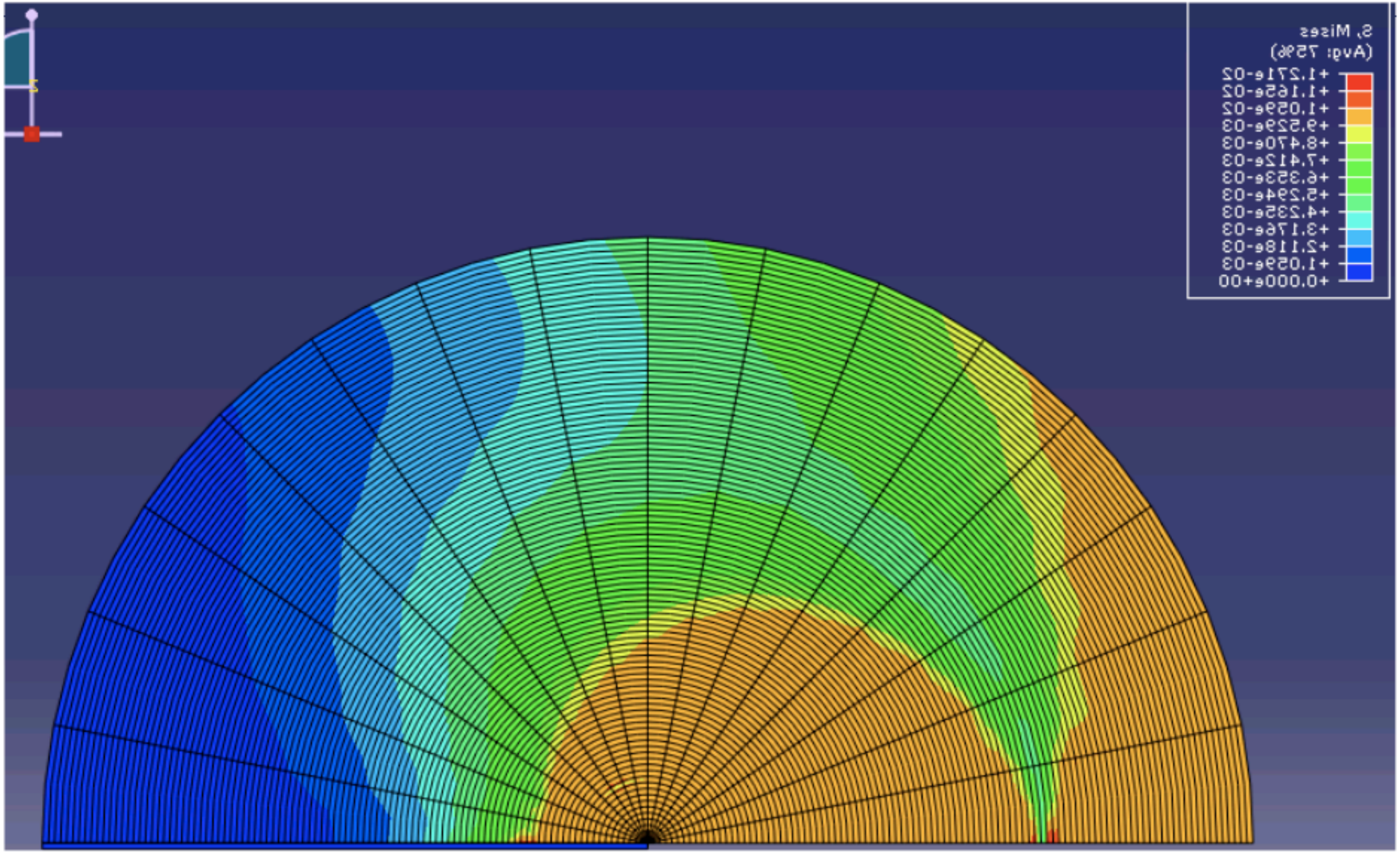

Conclusions

• Precipitates that grow at its edges obtain reduced pressure in its interior.

• At self-similar growth, stresses become logarithmically singular for all precipitates shapes.

• The mechanical state of the matrix of homogeneously growing precipitates matches the present solution exactly but for larger expansion.

• Spontaneous crack growth may occur